THE STABILITY AUGMENTATION SYSTEM FOR A HELICOPTER LANDING ON A VESSEL DECK

Marcin Żugaj, marcin.zugaj@pw.edu.pl, Warsaw University of Technology (Poland)

Sebastian Topczewski, sebastian.topczewski@pw.edu.pl, Warsaw University of Technology (Poland)

Przemysław Bibik, przemyslaw.bibik@pw.edu.pl, Warsaw University of Technology (Poland)

Adam Rosłowicz, Adam.Roslowicz@leonardocompany.com, „PZL-Świdnik" S.A. Leonardo Helicopters Company (Poland)

Jacek Małecki, Jacek.Małecki @leonardocompany.com, „PZL-Świdnik" S.A. Leonardo Helicopters Company (Poland)

Abstract
The paper presents part of the results obtained in the HELIMARIS project ("Modification of an optionally piloted helicopter for maritime mission performance") led by PZL Swidnik in cooperation with Warsaw University of Technology and CTO. In the paper, the automatic stability and augmentation system for helicopter landing on the moving vessel is presented. The model of the helicopter developed and evaluated in FLIGHTLAB software is using for analysis and synthesis of the control system algorithm. The simulation test on the system performances and robustness on the helicopter weight configuration as well as flight, environment and technical conditions are presented and discussed.

1. INTRODUCTION

Landing on a confined, moving vessel deck area is a very complicated and demanding task for a pilot, as helicopter handling qualities are influenced by several detrimental factors, such as [1],[2],[3]: environmental conditions; landing deck size and motion; limitations from the helicopter flight envelope and flying qualities. These factors make helicopter landing on a vessel deck a challenging task for a pilot, who may be supported by technology. The automatic control systems opens several opportunities to support the helicopter pilot during this mission [4],[5],[6].

A helicopter landing on a vessel deck is considered as composed of three stages: approach to a moving vessel, hover relative to a landing deck and final landing phase with touchdown. The objective of this research was to elaborate the Stability Augmentation System (SAS) to provide the satisfactory dynamic stability performance while performing the task, in both manual and automatic control modes [7].

This paper is a further development of work presented in [8] and [9].

The SAS for improving the robustness of light single engine helicopter is presented here. The SAS control laws are based on the classical control system design approach, and the analysis of the system resistance to the weight configuration and flight condition changes are introduced. The performances of the onboard devices and systems such as flight control system and sensors also contribute to the quality control and influence on the automatic flight control system performances. That is why the robustness of the proposed SAS system on the sensor noise, control system dead band and delay, and inflate the floats are also tested.

2. HELICOPTER DYNAMIC MODEL

The helicopter dynamic model is developed in FLIGHTLAB software and is based on

Presented at 47th European Rotorcraft Forum, United Kingdom, 7-9th September, 2021

PZL SW-4 helicopter configuration. It is a single rotor helicopter with one turboshaft engine, and classic configuration. Main rotor is articulated, three-bladed. Tail rotor is two-bladed, see-saw. All elements of the helicopter, except the undercarriage, are modeled as rigid. The main and tail rotors are modeled in a similar way, using blade element approach with flapping dynamics included. The aerodynamic model selected is quasi-steady with stall delay, and Peters-He 6 state induced velocity model. The interaction between rotors and fuselage are also modeled. The aerodynamic loads of the fuselage and empennage are modeled using empirical look-up tables. The engine model is based on FLIGHTLAB turboshaft engine model with detailed model of its dynamics and control systems. Coordinate systems used are described in [8]. The control system dynamic model is also included. The each servo-actuator is modeled as the nonlinear second order system, where the nonlinearities results from limits in actuator stroke, velocity and dead band.

3. CONTROL METHOD

The developed automatic flight control system consists of two independent closed loops (Figure 1). The outer loop i.e. Autopilot provides the short-term automatic control and stability of the attitude of the helicopter. The inner loop i.e. SAS improves the dynamic stability in both manual and automatic control. The several approach to design of the SAS control laws were analyzed, but the classical feedback control only attained a good review of the test pilots.

The presented SAS uses the classical feedback control method to improve the helicopter dynamic stability performance, and has the 10% of authority (Figure 2) [10]. The control system gains and wash-out filter parameters were obtained through detailed analysis of linear helicopter dynamic model for different flight conditions and mass configurations. Next, the SAS performances were investigated using the nonlinear helicopter dynamic model and a flight simulator, and the system parameters were tuned based on the test pilot remarks.

Table 1 Mean Quality Index for diff. weight

Weight config.	Mean QI		
	I_P	I_Q	I_R
Min.	32.1	26.0	18.0
Med.	23.4	19.4	11.1
Max.	41.3	24.4	8.9

The nonlinear helicopter model was also used to tests the robustness of the SAS on helicopter weight configuration, speed, turbulence, sensor noise, control system dead band and delay, and inflate the floats.

4. SIMULATION TESTS ON WEIGHT CONFIGURATION AND FLIGHT CONDITION

The simulation tests of the SAS quality control were performed using nonlinear helicopter model. The tests were done for three different helicopter mass configurations: minimum weight, medium weight and maximum weight, and different flight conditions: hover, forward flight with velocity at 10 m/s and 33 m/s. The rectangle impulse signal of amplitude of 5%, width 1s and initial time 1s was chosen as an test signal for each control channel i.e.: main rotor lateral cyclic pitch X_A, main rotor longitudinal cyclic pitch X_B, and tail rotor collective pitch X_P. The quality index I_ω was introduced to analyze the control quality. The index is formulated as a ratio of square quality indexes of angular velocities for SAS on and off configurations:

$$I_{\omega_i} = \frac{\int\left(\omega_{i\,SAS\,Off}\right)^2}{\int\left(\omega_{i\,SAS\,On}\right)^2}$$

where:

$\omega = \{P, Q, R\}$,

and P, Q, R are angular rates of roll, pitch and yaw respectively.

The examples of the system response for main rotor longitudinal pitch input and different weight configuration are shown in Figure 3, Figure 4, and Figure 5. The mean values of quality indexes for all weight and flight condition configurations are shown in the Table 1.

The results indicate that the angular velocity disturbances of the helicopter with the SAS are significantly smaller than that of a helicopter without the SAS. Moreover, it can be seen that the stabilization system provides the greatest improvement of stability in the roll channel, and the smallest in the yaw channel, and the greatest benefits of using the SAS are obtained in hover condition. As the airspeed increases, the natural stability of the helicopter improves, and the values of the quality index decrease. The tests also showed that after 20 seconds, in most cases, the helicopter without the SAS loses stability.

The next tests were performed for different wind and turbulence conditions for medium weight and without control excitation. The atmospheric effects for these tests were simulated using Dryden model, and the front-side wind blows at 5 m/s and 15 m/s

Presented at 47th European Rotorcraft Forum, United Kingdom, 7-9th September, 2021

from the direction of 45 deg were applied. The examples of the system response for main rotor longitudinal pitch input and different weight configuration are shown in Figure 6, Figure 7. The mean values of quality indexes for all flight conditions are shown in the Table 2.

Table 2 Mean Quality Index for diff. wind blows

Wind blow	Mean QI		
	I_P	I_Q	I_R
5 m/s	2.4	28.3	1.9
15 m/s	3.9	24.1	2.3

The results show that the SAS system reduces the angular velocity disturbances of the helicopter. The greatest improvement of stability can be seen in the pitch control channel.

5. SIMULATION TESTS ON TECHNICAL CONDITIONS

The quality of the automatic flight control system also depend on the technical conditions of the helicopter onboard devices and systems such as control system and sensors That is why the influence of the sensor noise, control system dead band and delay, and float conditions is presented here.

The measurement noises of gyroscopes were simulated as white noise, which were added to the measurement values of angular velocity signals. The three different variance values were investigated: 1 $(deg/s)^2$, 2 $(deg/s)^2$ and 10 $(deg/s)^2$. The examples of the system response for different flight conditions and excitation in X_B are shown in Figure 8 and Figure 9. The mean values of quality indexes for medium weight and all flight condition configurations are shown in the Table 3.

Table 3 Mean Quality Index for sensor noice

Variance	Mean QI		
	I_P	I_Q	I_R
1 $(deg/s)^2$	0,94	0,96	0,96
2 $(deg/s)^2$	0,85	0,91	0,92
10 $(deg/s)^2$	0,39	0,56	1,06

The results show that the low variance level do not influence significantly the system response. The variance at the level of 10 $(deg/s)^2$ causes the deficiency in the system response, mainly for the roll rate.

The control system dead band and delay were modeled as additional nonlinear elements in the servo-actuator dynamic model, which structure is shown in Figure 10. The actuator was modeled as the second order system with the nonlinear elements that comes from limits in actuator stroke (x_{max}) and velocity (V_{max}), dead band (Δx), and system delay (τ). The general equation of servo dynamic has form:

$$\begin{cases} \dot{x}_1 = x_2 \\ \dot{x}_2 = [u(t-\tau) - x_1] \cdot f(e) \cdot k_x - k_V \cdot x_2 \end{cases}$$

$$x = f_x(x_1)$$

where:

$$k_x = \omega_n^2$$

$$k_V = 2 \cdot \xi \cdot \omega_n$$

and the ω_n, ξ, u, and x are actuator natural frequency, damping ration, input and output signals respectively. The velocity and position integrals are limited according to the x_{max} and V_{max}. The functions reflecting the piston acceleration limit and backlash have forms:

$$f_e(e) = \begin{cases} -2V_{max} \cdot \xi/\omega_n & e \le -2V_{max} \cdot \xi/\omega_n \\ e & for\ \ |e| < 2V_{max} \cdot \xi/\omega_n \\ 2V_{max} \cdot \xi/\omega_n & e \ge 2V_{max} \cdot \xi/\omega_n \end{cases}$$

$$f_x(x_1) = \begin{cases} x_1 + \Delta x & x_{1\,switch} - x_1 \ge \Delta x \\ x_{1\,switch} & for\ \ |x_{1\,switch} - x_1| < \Delta x \\ x_1 - \Delta x & x_{1\,switch} - x_1 \le \Delta x \end{cases}$$

where $x_{1\,switch}$ is the piston position at the moment when it change the movement direction. The function $u(t-\tau)$ simulates the control system delay. The control signal is hold and stored in the buffer until the time delay τ, then it is sent to the actuator input.

The parameters of simulated servo-actuator are shown in the Table 4. According to the helicopter specification, the original flight control system has a dead band of 0.2 mm. Therefore, for the tests of the SAS, this value, double and half of this value were chosen, i.e.: 0.1 mm, 0.2 mm, 0.4 mm. In the case of the system time delay values, 10% of the time to reach the max stroke (0.013 s), and values two and four times smaller were assumed as the reference ones. However these values had to be correlated with the sample time of the simulation model solver. So, finally the selected values of the time delay were 0.0038s, 0.0076s, and 0.0152s.

Table 4 Servo-actuator data

Max stroke	*Max rate*	*Time to reach max stroke*
± *3 mm*	± 50 mm/s	0.13 s

The examples of the system response for different flight conditions and excitation in X_B are shown in Figure 11, Figure 12 for dead band and Figure 13,

Presented at 47th European Rotorcraft Forum, United Kingdom, 7-9th September, 2021

Figure 14 for time delay. The mean values of quality indexes for medium weight and all flight condition configurations are shown in the Table 5 for dead band and Table 6 for time delay.

The simulation results show that the assumed dead band values have a slight influence on the SAS performances. Noticeable differences appear only after 5 seconds of flight, and there are no differences in the nature of the transients but their amplitude. The results also show that the selected time delay values practically have no effect on the quality of the stabilization.

Table 5 Mean Quality Index for dead band

Dead band	Mean QI		
	I_P	I_Q	I_R
0.1 mm	1.3	1.0	1.8
0.2 mm	1.1	1.1	1.2
0.4 mm	1.0	1.2	0.9

Table 6 Mean Quality Index for time delay

Time delay	Mean QI		
	I_P	I_Q	I_R
0.0038 s	1,0	1,0	1,0
0.0076 s	1,0	1,0	1,0
0.0152 s	1,0	1,0	1,0

During these research the simulation model were used to test the impact of changes in the helicopter's aerodynamic characteristics, caused by the filling of the floats, on the SAS system performances. The tests were carried out for forward flight with speeds of 60 and 107 knots at a barometric altitude of 2000 ft. During the tests, the behavior of the helicopter was simulated when the SAS system was active at the moment of filling the floats and when its activation was delayed with 1 and 3 seconds. The time of inflate of the floats was 4 s.

The examples of the system response for cruise speed 60 knots and different SAS conditions (off, on, and on with delay of 1 and 3 seconds) are shown in Figure 15 and Figure 16.

The presented results show that the SAS system has limited influence on the helicopter behavior after inflate the floats. This is because this system is designed to improve the dynamic stability of the helicopter i.e. to minimize disturbances in steady flight. Inflation of the floats do not cause sudden disturbances, but rather a gradual deviation from the equilibrium state caused by the change of the aerodynamic characteristics. In the initial time, the dynamics of this phenomenon is even significant and the SAS system compensates its effect. Later the continuously attitude deviation that cannot be compensated by the SAS can be observed, because this task should be performed by the pilot or autopilot. That is why the tests were repeated and the autopilot attitude hold mode was engaged. The results are shown in Figure 17 and Figure 18, and indicated that the SAS system effectively suppresses undesirable disturbances and the autopilot maintains the orientation resulting from trimming conditions before filling the floats.

The delay in the activation of the SAS system has small effect on the behavior of the helicopter. In the case of a delay time of 1 second, the SAS effect is practically imperceptible. For a delay time of 3 seconds, the difference is visible but small.

6. CONCLUSIONS

In the paper the stability and augmentation system for helicopter landing on a moving vessel's deck was presented. The nonlinear simulation model was used for analysis and synthesis of the control laws. The tests for the system robustness on the helicopter weight configuration as well as flight, environment, and technical conditions were presented.

The developed stability control system utilized the classical control method and provided good handling qualities which was confirmed by the test pilots during test on the flight simulator.

The simulation tests of the system performance covered different helicopter weight configuration, speed, wind blows, measurement system noise, control system dead band and time delay, and floats conditions. The results of the tests confirmed the good performances of the system in alleviation of the flight disturbances.

7. ACKNOWLEDGMENTS

Research conducted as part of the INNOLOT sector project (acronym HELIMARIS) entitled "Modification of an optionally piloted helicopter to maritime mission performance" coordinated by Wytwórnia Sprzętu Komunikacyjnego "PZL-Świdnik" Spółka Akcyjna, co-financed by the National Centre for Research and Development under the Smart Growth Operational Programme 2014-2020, 1. Priority Axis, Support for R&D activity of Enterprises; Action 1.2, Agreement No. POIR.01.02.00-00.0004/15.

8. REFERENCES

[1]Topczewski S., Narkiewicza J., Bibik P., „Helicopter Control During Landing on a Moving Confident Platform", IEEE Access, Vol. 8, pp. 107315-107325, June 2020

[2]McCallum A.T., Buchanan R., Woodrow I., „Modelling of an Autonomous MUAV at the Ship Dynamic Interface Within a Multinational Simulation Framework", 28th European Rotorcraft Forum, Bristol, UK, 17-20 September 2002

[3]Ngo T.D., „Constrained Control for Helicopter Shipboard Operations and Moored Ocean Current Turbine Flight Control", Virginia Polytechnic Institute and State University, USA, March 2016

[4]Holmes W., Langelaan J., „Autonomous Shipboard Landing using Monocular Vision", American Helicopter Society 72nd Annual Forum, West Palm Beach, Florida, USA, 17-19 May 2016

[5]Fourie C.K., „The Autonomous Landing of an Unmanned Helicopter on a Moving Platform", Stelenbosch University, USA, 2015

[6]Sandino A., Bejar M., Ollero A., „On the applicability of linear control techniques for autonomous landing of helicopters on the deck of a ship", IEEE International Conference on Mechatronics, Istanbul, Turkey, 13-15 April 2011

[7]Horn J., Bridges D., „A Model Following Controller Optimized for Gust Rejection during Shipboard Operations", American Helicopter Society 63rd Annual Forum, Virginia Beach, VA, 1-3 May 2007

[8]Bibik P., Topczewski S., Żugaj M., „Development of an Automatic System for Helicopter Approach to a Moving Vessel," 44th European Rotorcraft Forum, Delft, Netherlands, 18-20 September 2018

[9]Topczewski S., Bibik P., Narkiewicz J.: The Final Phase of a Helicopter Automatic Landing on a Vessel Deck, 45th European Rotorcraft Forum, Warsaw, Poland, 17-20 September, 2019

[10]McLean D.: Automatic flight control systems, Prentice Hall, New York, 1990

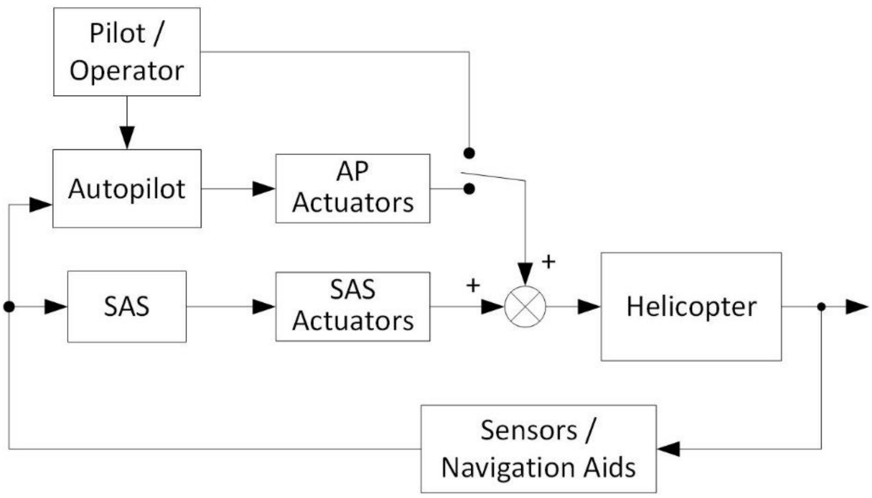

Figure 1 Helicopter control system architecture

Presented at 47th European Rotorcraft Forum, United Kingdom, 7-9th September, 2021

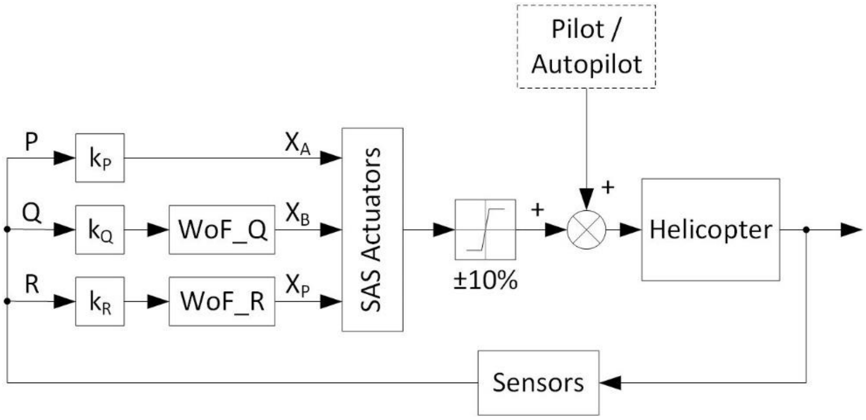

Figure 2 SAS control laws structure

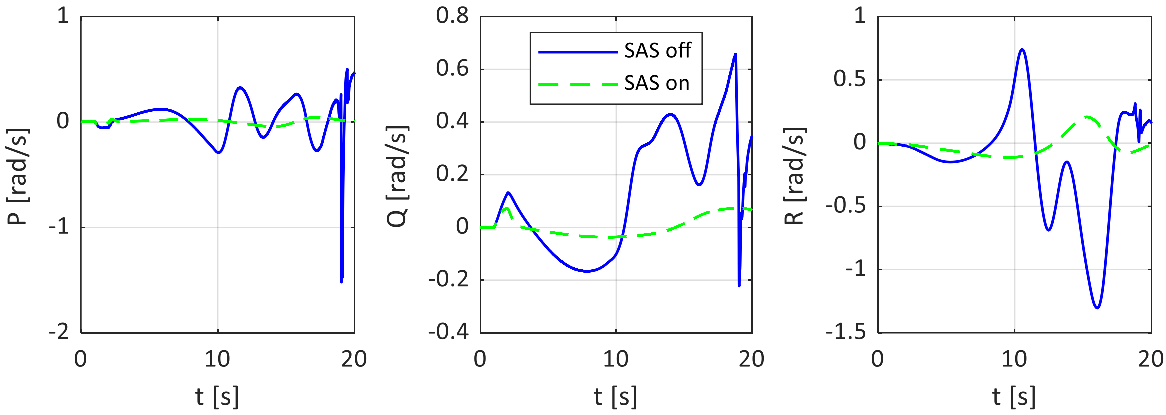

Figure 3 System time response for exitation of X_B, hover condition, min. weight

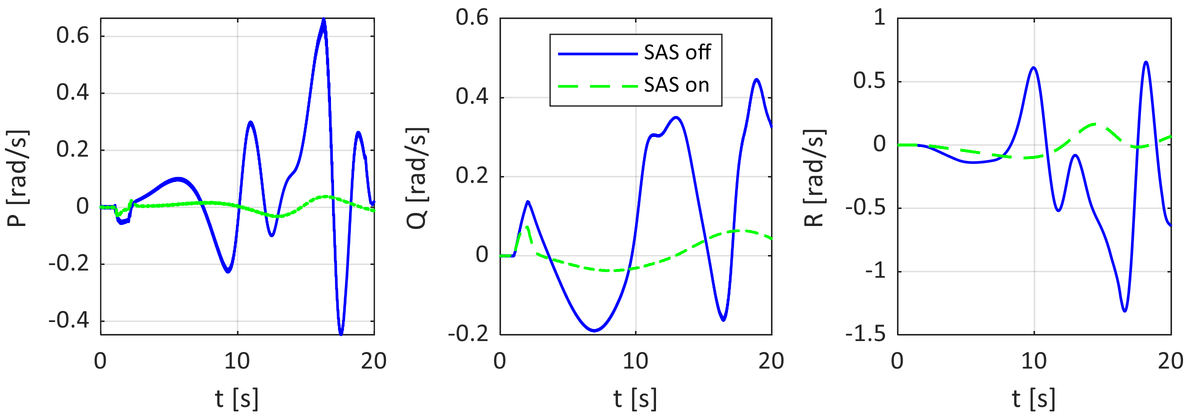

Figure 4 System time response for exitation of X_B, hover condition, med. weigh

Presented at 47th European Rotorcraft Forum, United Kingdom, 7-9th September, 2021

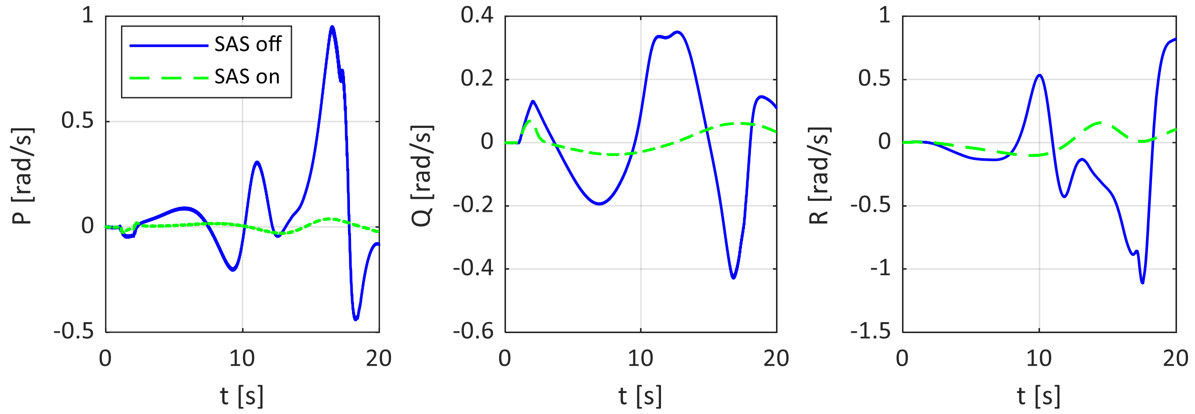

Figure 5 System time response for exitation of X_B, hover condition, max. weight

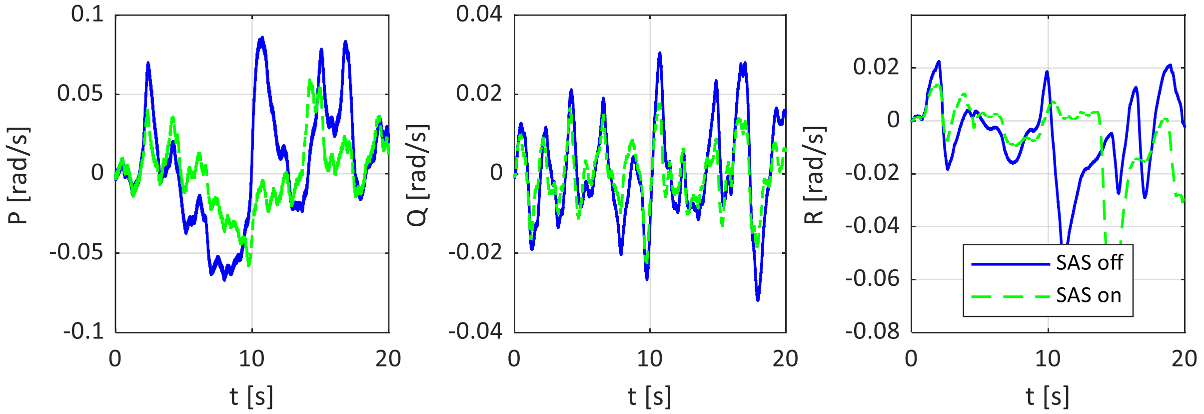

Figure 6 System time response for wind blows 5 m/s, cruise at 33 m/s, med. Weight

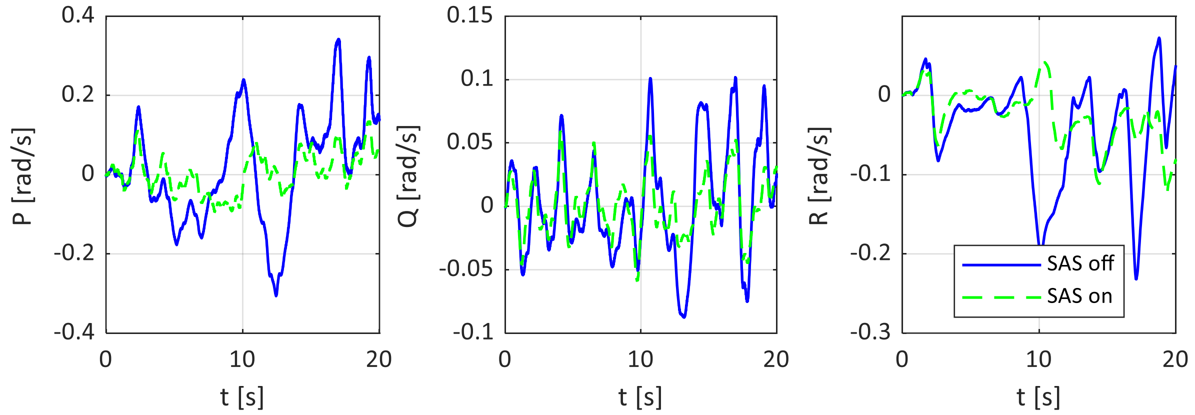

Figure 7 System time response for wind blows 15 m/s, cruise at 33 m/s, med. weight

Presented at 47th European Rotorcraft Forum, United Kingdom, 7-9th September, 2021

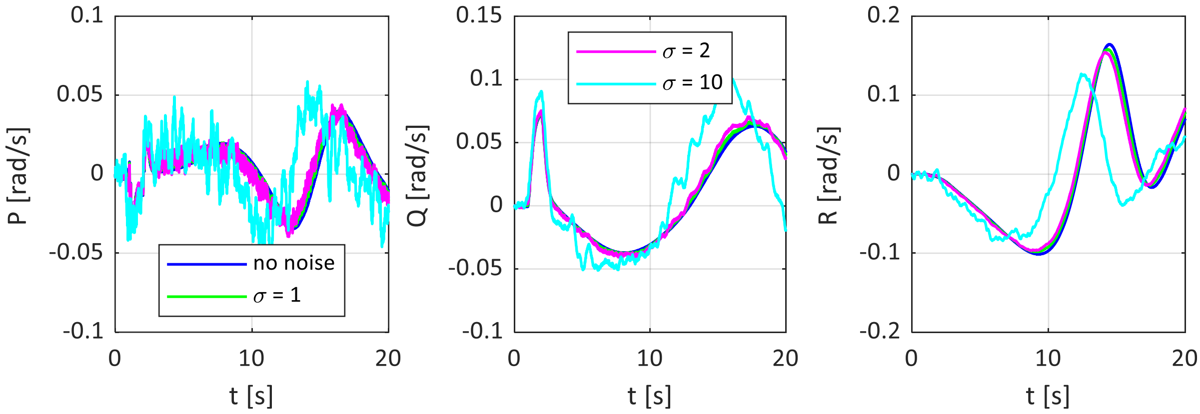

Figure 8 System time response for different sensor noise, hover condition, med. weight

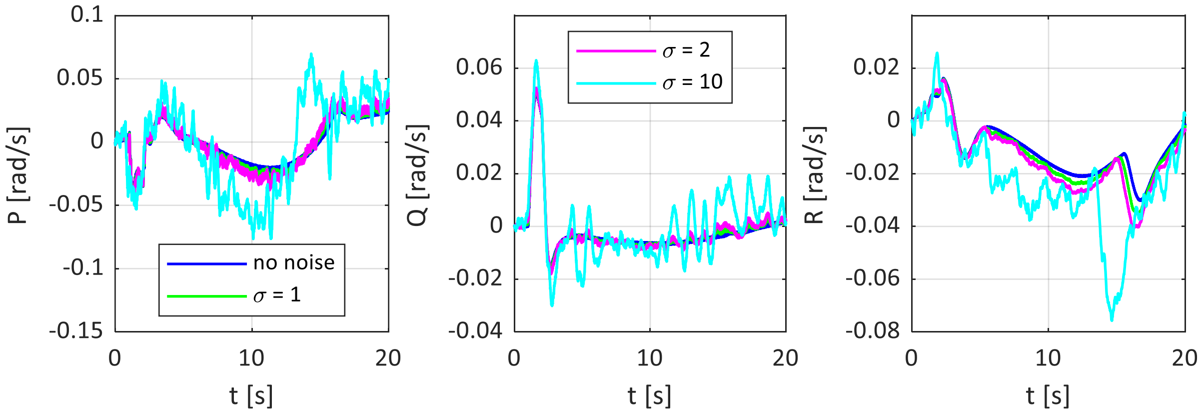

Figure 9 System time response for different sensor noise, fowar flight at v=33 m/s, med. weight

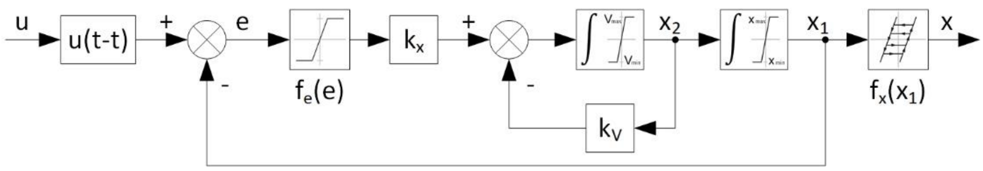

Figure 10 Structure of the flight control system

Presented at 47th European Rotorcraft Forum, United Kingdom, 7-9th September, 2021

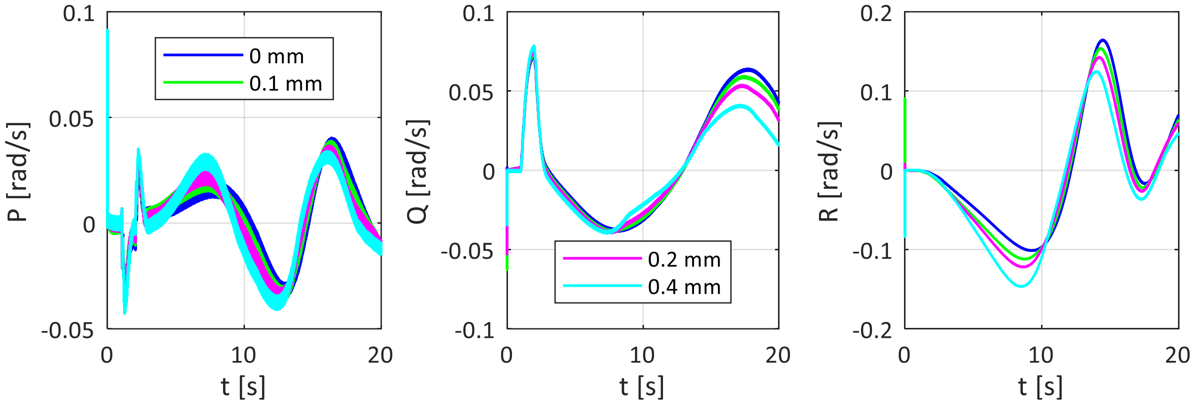

Figure 11 System time response for different dead band, hover condition, med. weight

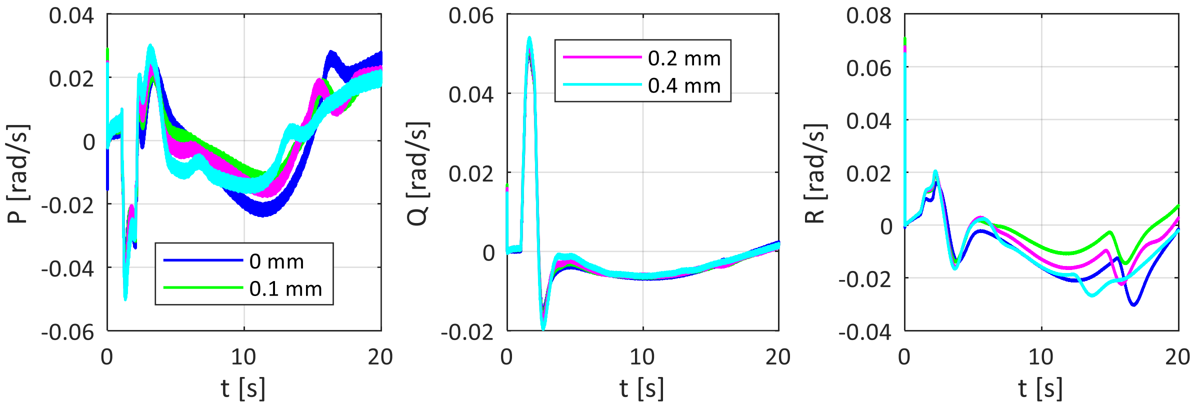

Figure 12 System time response for different dead band, fowar flight at v=33 m/s, med. weight

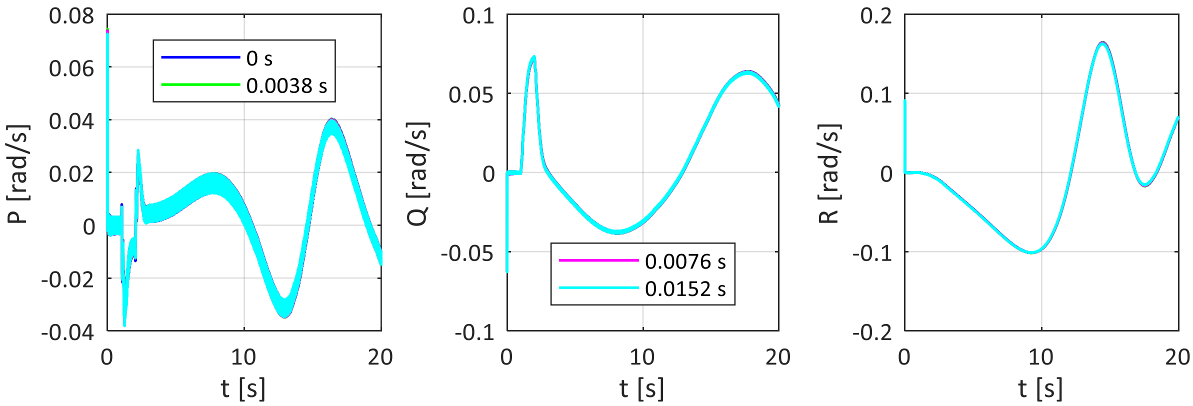

Figure 13 System time response for different time delay, hover condition, med. weight

Presented at 47th European Rotorcraft Forum, United Kingdom, 7-9th September, 2021

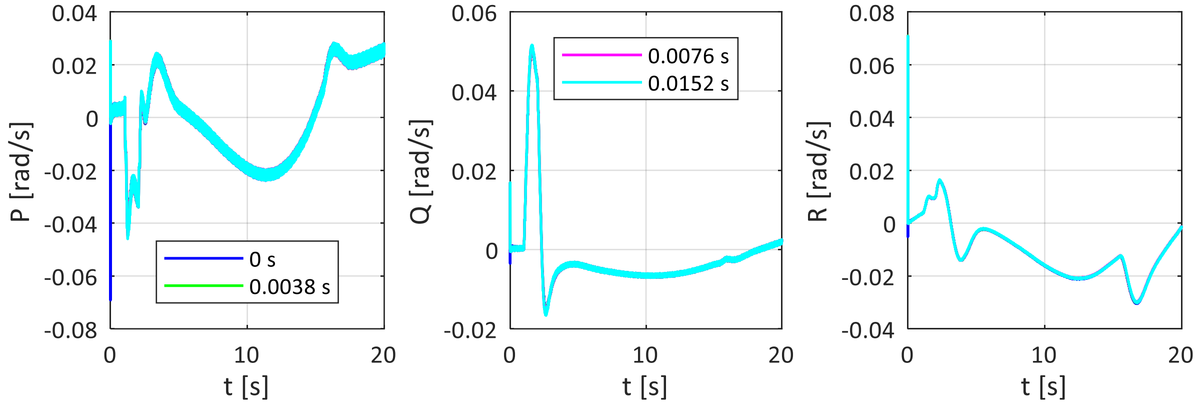

Figure 14 System time response for different time delay, fowar flight at v=33 m/s, med. weight

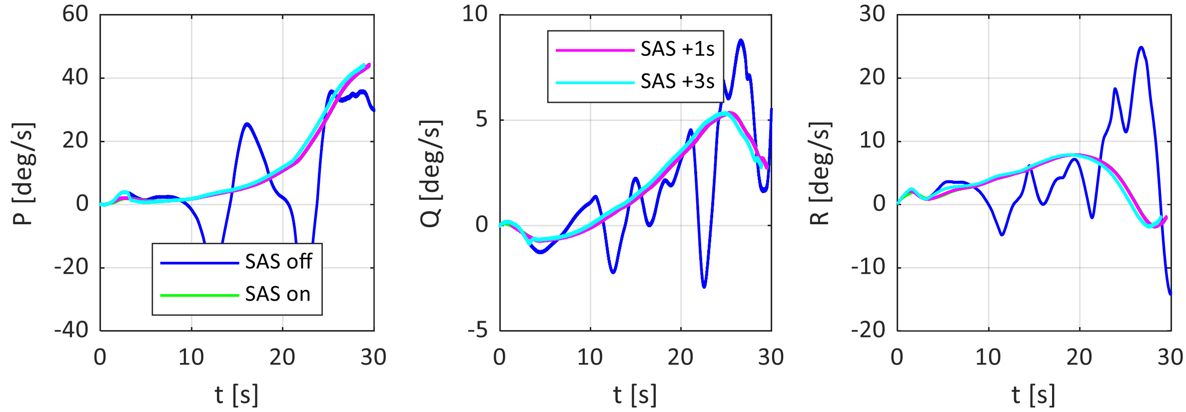

Figure 15 Angular rate after floats inflation, cruise at 60 kn, med. weight

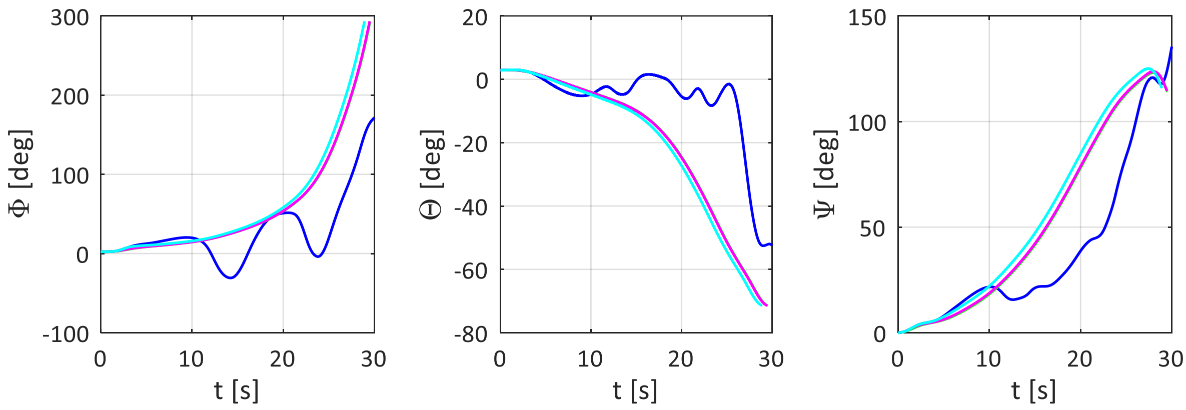

Figure 16 Attitude after floats inflation, cruise at 60 kn, med. Weight

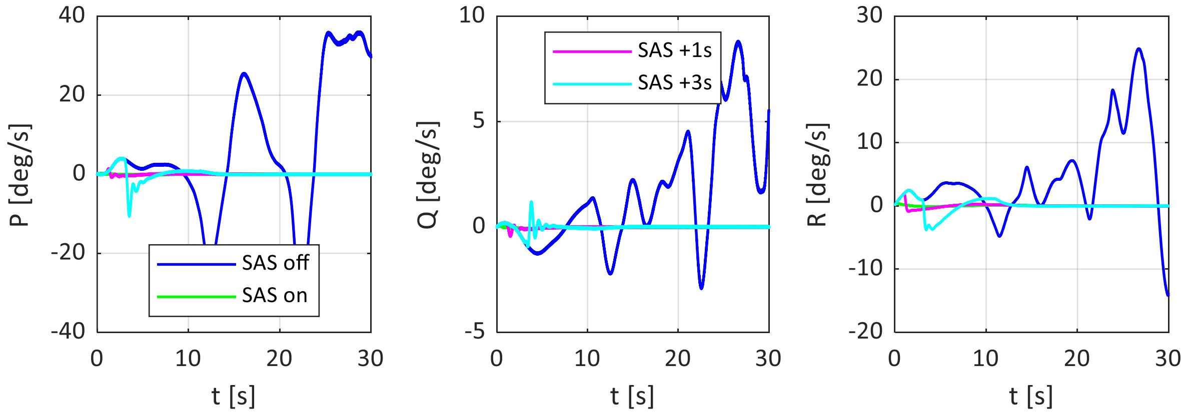

Figure 17 Angular rate after floats inflation, autopilot engaged, cruise at 60 kn, med. weight

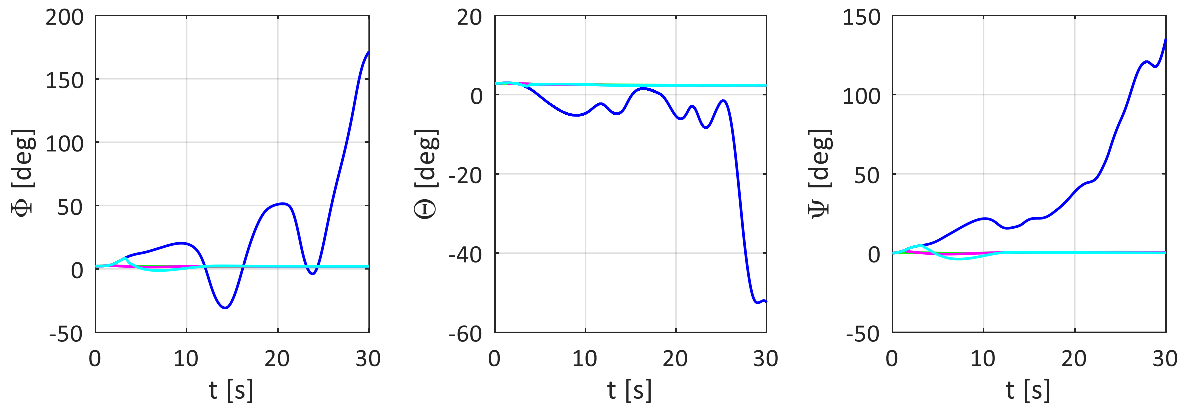

Figure 18 Attitude after floats inflation, autopilot engaged, cruise at 60 kn, med. Weight

Presented at 47th European Rotorcraft Forum, United Kingdom, 7-9th September, 2021